ISSN (e): 2250 – 3005 || Volume, 08 || Issue, 2|| February – 2018 ||
International Journal of Computational Engineering Research (IJCER)

# The Effect of Annealing Temperature on the Physical Properties of Electron Beam Evaporated Cuprous Oxide Thin Films

V. Sravanthi[1], T. Srikanth[1], R. Subba Reddy[1], A. Sivasankar Reddy[1]*, P. Sreedhara Reddy[2],
B. Radha Krishna[3], Ch. Seshendra Reddy[4]
[1]Department of Physics, Vikrama Simhapuri University P.G. Centre, Kavali -524201, A.P., India
[2]Department of Physics, Sri Venkateswara University, Tirupati- 517502, A.P., India
[3]Department of Physics, NBKR Institute of Science and Technology, Vidyanagar-524413, India
[4]Department of Materials Science and Engineering, Harbin Institute of Technology, University Town, Shenzhen, 518055, China
Corresponding author: A. Sivasankar Reddy

**ABSTRACT**
Cuprous oxide ($Cu_2O$) thin films were prepared on glass substrates using electron beam evaporation and studied the effect of annealing temperature on the compositional, structural, microstructural, electrical and optical properties. From the XRD results, (111) is preferred orientation and polycrystalline nature increases with annealing temperature. The obtained lattice parameter values are lower than the bulk value. By increasing the annealing temperature the grains grew much bigger and islands also appeared. The electrical resistivity and optical band gap of the films decreases with increasing of annealing temperature.
**KEYWORDS:** Cuprous Oxide, Thin Films, Electron beam evaporation, Temperature

## I. INTRODUCTION

Cuprous oxide($Cu_2O$) is p-type semiconductor with direct band gap of 2.1 eV, non-toxicity, low production cost and high absorption coefficient, used in solar cells, sensor arrays, batteries, transparent displays, energy converting devices [1-7]. In the literature, various thin film deposition methods such as electrochemical deposition [8], chemical vapour deposition [9], spray pyrolysis [10], magnetron sputtering [11], and electron beam evaporation [12] have been attempted for the deposition of $Cu_2O$ films. In the literature, very few reports on the electron beam evaporated $Cu_2O$ films. Electron beam evaporation (EBE) is an efficient technique for the thin film growth because of material loss is minimal, uniformity of the films over the substrate, useful for depositing alloy and compound materials, films having the stoichiometry close to the bulk. In the present investigation, the $Cu_2O$ films were prepared on the glass substrates and studied the effect of annealing temperature on the physical properties of the films.

## II. EXPERIMENTAL

The $Cu_2O$ thin films were deposited on the glass substrates by electron beam evaporation using $Cu_2O$ pellets. The vacuum system is capable of creating an ultimate vacuum of $4x10^{-4}$ Pa. the vacuum chamber was pumped with the combination of diffusion pump and rotary pump. The pressure was measured using a Pirani–Penning gauge combination. The pellet was prepared using high purity (99.99%) $Cu_2O$ powder. The pellets were kept in a water-cooled copper crucible. The thickness of the films was monitored by quartz crystal thickness monitor and the thickness of the films was around ~190 nm. The films deposited on unheated substrate (~303K) and subsequently post-annealed at different temperatures (373, 573K and 673K) in air. The deposition parameters maintained during the preparation of $Cu_2O$ films are given in Table 1.

The chemical composition of the films was analyzed by Energy Dispersive Spectroscopy (EDS) attached with SEM of model Oxford instruments Inca Penta FET X3. The crystallographic structure of the films was analyzed by Seifert 3003TT X-ray diffractometer (XRD), using Cu Kα radiation (k = 0.1546nm). The microstructure and surface morphology of the films was studied by scanning electron microscopy (SEM) and atomic force microscopy (AFM), respectively. The optical transmittance of the films was recorded using a UV–Vis–NIR double beam spectrophotometry. The electrical properties of the films were measured by using standard four-probe method.

Table.1. Deposition parameters of $Cu_2O$ films during deposition

| | |
|---|---|
| Deposition method | : electron beam evaporation |
| Power source | : e-beam power supply (3kW) |
| Pellet | : $Cu_2O$ (10mm dia and 3mm thick) |
| Substrates | : Glass |
| Target to substrate distance | : 60 mm |
| Ultimate pressure ($P_U$) | : $4x10^{-4}$ Pa |
| Evaporation pressure ($P_W$) | : $3x10^{-2}$ Pa |
| Substrate temperature ($T_S$) | : 303K |
| Accelerating voltage | : 4 kV |
| Filament current | : 30 mA |
| Deposition time | : 8 to 12 min |

## III. RESULTS AND DISCUSSION

**Fig.1.** shows the EDS spectra of electron beam evaporated $Cu_2O$ films at different annealing temperatures. From the EDS results, no reflections of impurity were detected and obtained composition results were listed in Table 2. The as deposited films show high oxygen content and it decreased after elevating the annealing temperature.

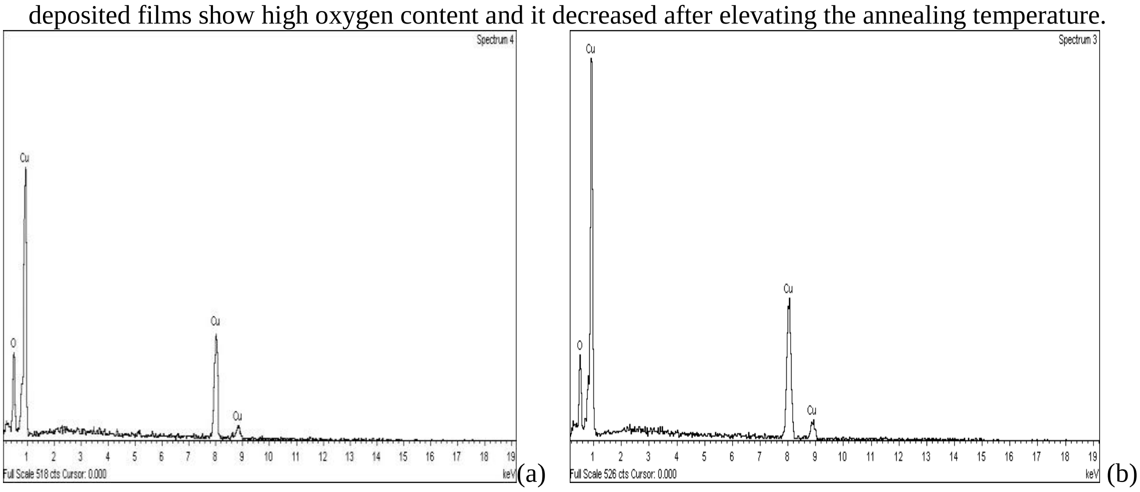


**Fig. 1. EDS spectra of $Cu_2O$ films (a) as deposited(373 K) and (b) annealed films(673K)**

**Table 2: The compositional results of $Cu_2O$ films by Energy Dispersive Spectroscopy (EDS)**

| Sample history | Element | Atomic percentage |
|---|---|---|
| As deposited (303K) | O K | 37.12 |
| Annealing temperature of 673K | Cu K | 62.88 |
| | O K | 34.83 |
| | Cu K | 65.17 |

### 3.1 Structural properties

The crystallinity of the films was highly influenced by annealing temperatures. Fig.2. shows the XRD patterns of $Cu_2O$ films at different annealing temperatures. The as deposited films (303K) exhibited broad peak and corresponding to (111) orientation of $Cu_2O$. The peak width decreased after annealed the films at 373K. On further increasing the annealing temperature, cyrstallinity and peak intensity of the films was increased greatly and an additional peak of (200) was appeared along with (111) orientation. At low temperature the vapour species have low surface mobility and it prevent the full crystallization of the films[13] hence, the films exhibited poor crystallinity.

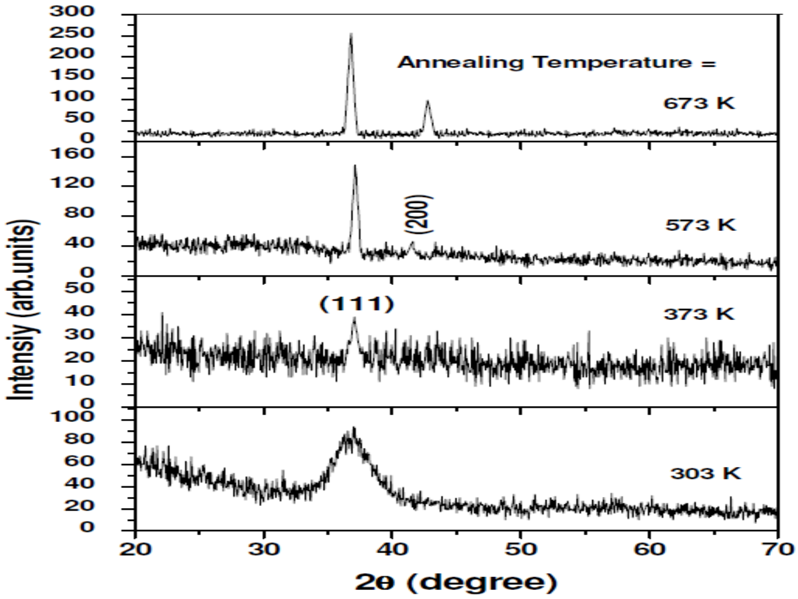


**Fig. 2. XRD patterns of $Cu_2O$ films at different annealing temperatures**

The crystallite size of films was increases more rapidly at higher annealing temperatures. The average crystallite size of films was calculated by using Scherrer's equation [14], and listed in Table 3. Sravanan et al. [15] observed the crystallite size increased with annealing temperature due to the coalescence of smaller grains by the improving in the thermal agitation of the lattice.

The dislocation density (δ) of the films is defined as the length of dislocation lines per unit volume and was calculated by the following equation [16],

$$\delta = 1/D^2 \qquad \text{----------- (1)}$$

The dislocation density (δ) of the films decreased with increasing of annealing temperature (Table 3), indicating the reduction of lattice defects and grain boundaries.

The lattice parameter (a) of the films was calculated using the following relation

$$d = a / (h^2+k^2+l^2)^{1/2} \qquad \text{-----------(2)}$$

where h, k and l are the Miller indices. The interplaner spacing (d) was calculated from the X-ray diffraction data using the Bragg's relation. The lattice parameter of the films increased with increasing of the annealing temperature (Table 3) and the obtained lattice parameter values are lower than the standard value (ICDD = 4.269**Å)**. Wang et al. [17] observed that the decreasing of the lattice parameter with increasing the annealing temperature in rf magnetron sputtered $Cu_2O$ films.

**Table 3: Crystallite size, dislocation density, lattice parameters and RMS roughness values of $Cu_2O$ films at different annealing temperatures.**

| Annealing temperature | Crystallite Size (nm) | Dislocation density (lines/nm$^2$) | Lattice parameter (Å) | RMS roughness (nm) |
|---|---|---|---|---|
| 303K | 5 | $4.0 \times 10^{-2}$ | 4.147 | 5.6 |
| 373K | 12 | $6.9 \times 10^{-3}$ | 4.205 | 4.9 |
| 573K | 20 | $2.5 \times 10^{-3}$ | 4.233 | 4.1 |
| 673K | 26 | $1.5 \times 10^{-3}$ | 4.241 | 3.6 |

### 3.2. Microstructure and surface morphology

The SEM images of $Cu_2O$ films at different annealing temperatures are shown in Fig.3. The as deposited films exhibited small grains and islands due to large number of structural defects and lattice disorder. After annealed the films the microstructural defects are reduced and consequently grain size becomes bigger and uniform.

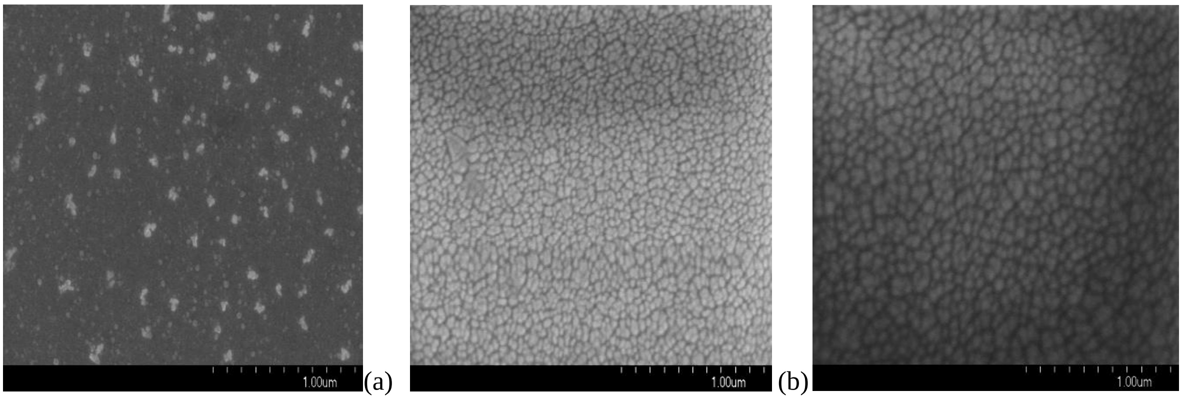


**Fig.3. SEM images of $Cu_2O$ films at different annealing temperatures: (a) 303K, (b) 573K and (c) 673K**

The surface morphology of films was strongly influenced by the annealing temperature. Fig.4. shows the three-dimensional AFM images of $Cu_2O$ films at different annealing temperatures. From the images, the films deposited at room temperature exhibited smaller grains with irregular shapes and grain islands. By increasing the annealing temperature the grains grew much bigger and islands also appeared. The root mean square (RMS) surface roughness of films was measured and listed in Table 3. The roughness of the films decreases gradually with increasing the annealing temperature. This was due to improvement of the crystallinity and reduction of the grain boundaries.

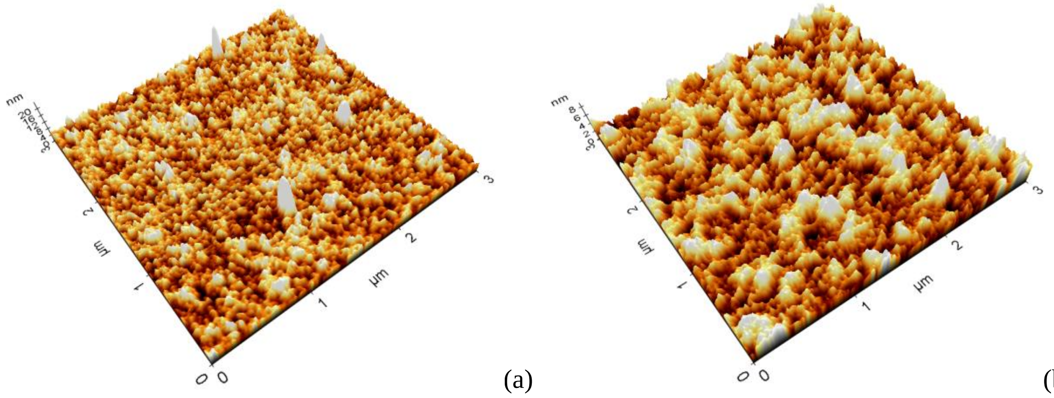


**Fig.4. AFM images of $Cu_2O$ films (a) as deposited (303K), (b) annealing temperature of 673K**

### 3.3. Electrical and Optical properties

The electrical properties of the films are very sensitive to the structural defects and surface roughness. The electrical properties of $Cu_2O$ films at different annealing temperatures are listed in Table 4. The electrical resistivity and carrier concentration of the films decreases whereas, mobility increases with increasing of the annealing temperature. Li et al. [18] observed that the Hall mobility of $Cu_2O$ films increases with increasing of annealing due to diffusion of oxygen atoms or grains or defect passivation during annealing process.

It is known that the optical properties of the films are highly influenced by the density of defects, crystallinity and surface roughness of the films. Fig.5. shows the optical transmittance spectra of $Cu_2O$ films at different annealing temperatures. The optical transmittance of the films increases with increasing annealing temperature from 303K to 573K and decreases at higher temperature of 673K. This was may be due to increasing of the oxygen vacancies at higher temperatures. The absorption edge of the films shifted higher wavelength side with the increase of annealing temperature.

The optical band gap ($E_g$) of the films was evaluated from the extrapolation of the linear portion of the plots of $(\alpha h\nu)^2$ versus ($h\nu$) ($\alpha$ is the absorption coefficient, $h\nu$ is the photon energy). The obtained optical band gap values of $Cu_2O$ films at different annealing temperatures are listed in Table 4. The band gap decreases from 2.37 to 2.27eV with increasing of annealing temperature. The decreasing of band gap values with increases of annealing temperature was due to reduction of structural defects and enhancement of crystallinity of the films.

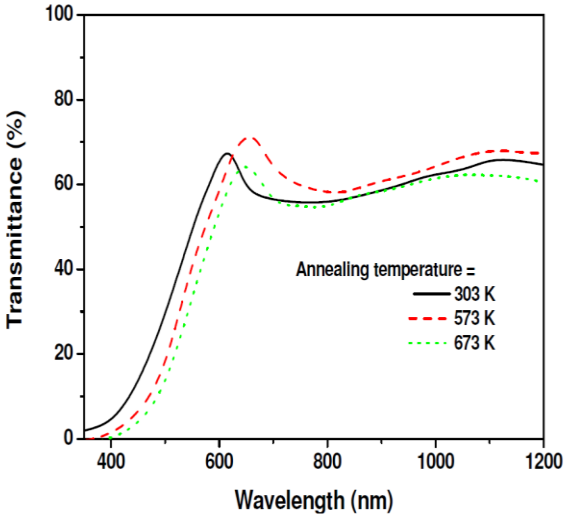


**Fig.5. Optical transmittance spectra of $Cu_2O$ films**

**Table 4. Electrical and optical properties of $Cu_2O$ films at different annealing temperatures($T_a$)**

| Sample History | Resistivity (Ωcm) | Hall mobility ($cm^2/V.sec$) | Carrier concentration ($cm^{-3}$) | Transmittance (%)at λ=650 nm | Band gap (eV) |
|---|---|---|---|---|---|
| **$T_a$ =** | | | | | |
| 303K | 82 | 1.8 | $4.2x10^{16}$ | 61 | 2.37 |
| 573K | 49 | 5.4 | $2.4x10^{16}$ | 70 | 2.31 |
| 673K | 38 | 11 | $1.5x10^{16}$ | 65 | 2.27 |

## IV. CONCLUSIONS

$Cu_2O$ thin films have been deposited on glass substrates using electron beam evaporation. The films exhibited only $Cu_2O$ phase, no impurities such as Cu, CuO was observed. The microstructure and surface morphology of the films improved with annealing temperature. At the annealing temperature of 573K the films exhibited highest transmittance of 70% with electrical resistivity of 49Ωcm. The optical band gap of the films decreased from 2.37 to 2.27eV with increasing of annealing temperature.

## REFERENCES


[1]. H.Y. Xu, J.K. Dong, C. Chen, Materials Chemistry and Physics 143:713, 2014.
[2]. J. Gan, S. Gorantla, H. N. Riise, Ø. S. Fjellva, S. Diplas, O. M. Løvvik, B. G. Svensson, E. V. Monakhov, E. Gunnæs, Applied Physics Letters 108:152110, 2016.
[3]. J. Xue, Q. Shen, W. Liang, X. Liu, L. Bian, B. Xu, Surf. Coat. Techno. 216:166, 2013.
[4]. D. Barreca, E. Comini, A. Gasparotto, C. Maccato, C. Sada, G. Sberveglieri, E. Tondello,
[5]. Sensors Actuators B Chem. 141:270, 2009. C.L. Hsu, J.Y. Tsai, T.J. Hsueh, Sens. Actuators B 224:95, 2016.
[6]. F. Hu, K.C. Chan, T.M. Yue, C. Surya, Thin Solid Films 550:17, (2014).
[7]. H.A. Al-Jawhari, Mater. Sci. Semicond. Process. 40:241, 2015.
[8]. A. Ashida, S. Sato, T. Yoshimura, N. Fujimura, J. Crystal Growth, 468:245, 2017.
[9]. S. Eisermann, A. Kronenberger, A. Laufer, J. Bieber, G. Haas, S. Lautenschlager, G. Homm, P.J. Klar, B.K. Meyer, Phys. Status Solidi A 209:531, 2012.
[10]. R.D. Prabu, S. Valanarasu, I. Kulandaisamy, V. Ganesh, Mohd Shkir, A. Kathalingam, J Mater Sci: Mater Electron 28:6754, 2017.
[11]. H. Sun, S-C. Chen, C-K. Wen, T-H.Chuang, M.A.P. Yazdi, F. Sanchette, A. Billard, Ceramics International 43:6214, 2017.
[12]. R. Oommen1, U. Rajalakshmi, Sanjeeviraja, Int. J. Electrochem. Sci., 7:8288, 2012.
[13]. ZW Chen, JKL. Lai, CH. Shek, J Non-Cryst Solids 355:2647, 2009.
[14]. B.D. Cullity, Elements of X-ray Diffraction, second ed., Addison Wesley, London
[15]. V. Saravanan, P.Shankar, G.K. Mani, J.B.B.Rayappan Journal of Analytical and Applied Pyrolysis 111:272, 2015.
[16]. H.P. Klug, L.E. Alexander, X-Ray Diffraction Procedures for Polycrystalline and Amorphous Materials, Wiley, NewYork, 1974.
[17]. Y. Wang, P. Miska, D. Pilloud, D. Horwat, F. M€ucklich, J. F. Pierson, J. Appl. Phys. 115:073505, 2014.
[18]. F.M. Li, R. Waddingham, W.I. Milne, A.J. Flewitt, S. Speakman, J. Dutson, S. Wakeham, M. Thwaites, Thin Solid Films 520:1278, 2011.


V. Sravanthi " The Effect of Annealing Temperature on the Physical Properties of Electron Beam Evaporated Cuprous Oxide Thin Films” International Journal of Computational Engineering Research (IJCER), vol. 08, no. 02, 2018, pp. 59-63.